Supplementary Information (SI) for Nanoscale.
This journal is © The Royal Society of Chemistry 2025

*Supporting Information*

# Surface palladium nanoparticles in ionic liquids modified with phosphorus ligands for enhanced catalytic semi-hydrogenation

Muhammad I. Qadir [a]*, Gustavo Chacón-Rosales [b,c]*, Camila P. Ebersol [a], Gabriel Abarca [b], Pedro H. F. Matias [a], Heibbe Cristhian. B. de Oliveira [a], Renato B. Pontes [d], Rafael Stieler [e], and Jairton Dupont [e,f]*

[a] Instituto de Química-Universidade Federal de Goiás-UFG-Av. Esperança s/n, Campus Samambaia, 74690-900, Goiânia, Goiás, Brazil.
[b] Universidad Bernardo O´Higgins, Centro Integrativo de Biología y Química Aplicada (CIBQA), Facultad de Ciencias de la Salud, General Gana 1702, Santiago, Chile.
[c] Instituto de Tecnología Química, Universitat Politècnica de València-Consejo Superior de Investigaciones Científicas, Av. de los Naranjos s/n, 46022 Valencia, Spain.
[d] Instituto de Fisica-Universidade Federal de Goiás-UFG-Av. Esperança s/n, Campus Samambaia, 74690-900, Goiânia, Goiás, Brazil.
[e] Instituto de Química, Universidade Federal Do Rio Grande Do Sul, Porto Alegre, RS, 91509-900, Brazil.
[f] Departamento de Bioquímica y Biología Molecular B e Inmunología Facultad de Química, Universidad de Murcia, P.O. Box 4021, E-30100 Murcia, Spain.

## 1. Synthesis of Pd(II) complex

In a general procedure, $PdCl_2$ (0.27 g; 1.5 mmol) was dissolved in hot concentrated hydrochloric acid (4 mL) to generate in situ $H_2[PdCl_4]$. This solution was diluted in dry ethanol (40 mL), filtered off and the filtrate was added to a solution of the corresponding 3-(3-(diphenylphosphaneyl)propyl)-1,2-dimethyl-1*H*-imidazol-3-ium bis((trifluoromethyl)sulfonyl) amide (2.5 equivalents) previously dissolved in ethanol under argon atmosphere. The mixture was stirred vigorously during 16 h obtaining a pale yellow solid, which was filtered off and washed with successive portions of ethanol, water and ethanol (3 x 5 mL), then was dried under vacuum.

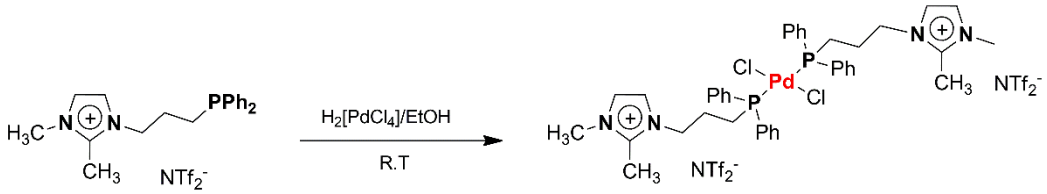

## 2. $^{31}$P-NMRs of ionophilic phosphine and Pd(II) complex

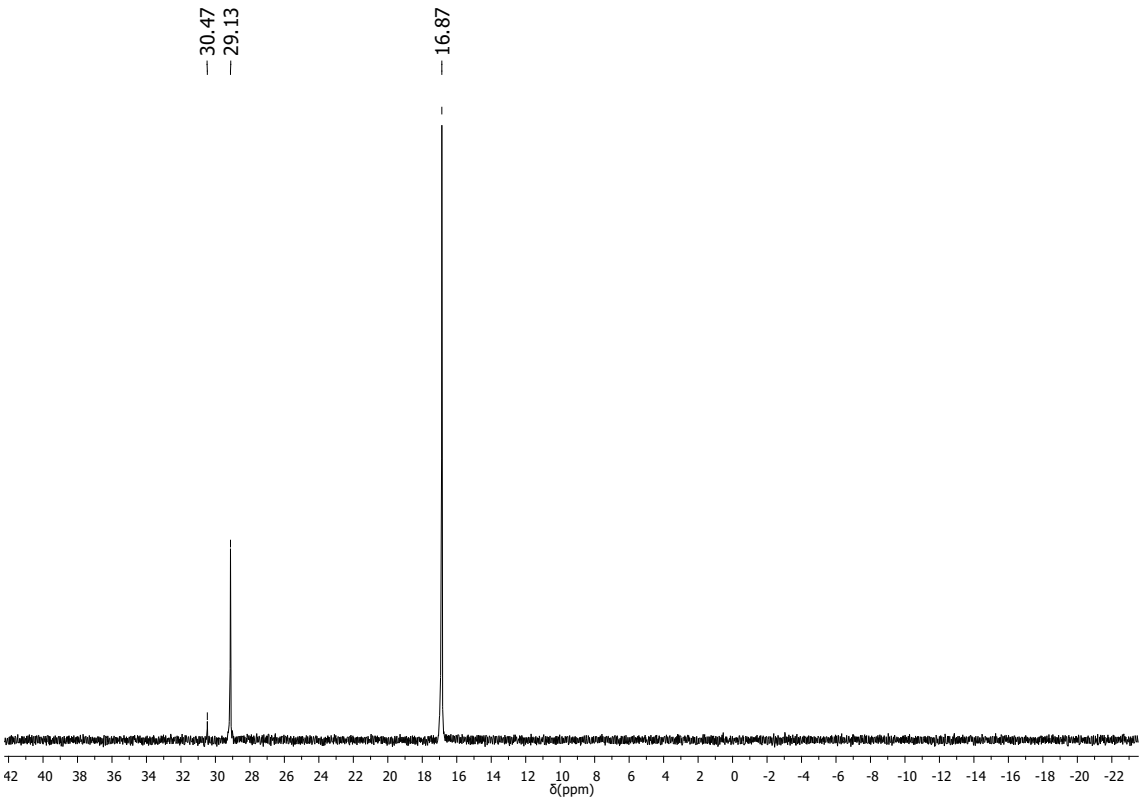


**Figure S1.** $^{31}$P-NMR spectrum of our Pd (II) complex in DMSO-$d_6$.

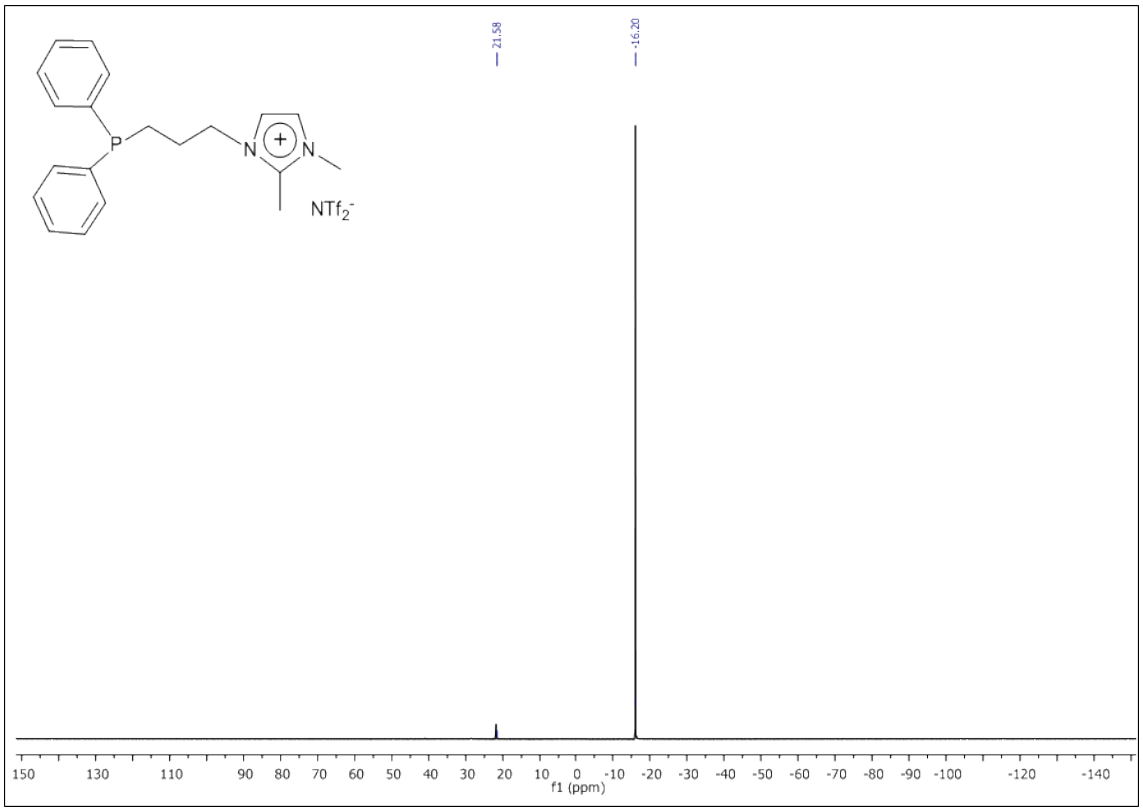


**Figure S2.** $^{31}$P-NMR spectrum of ionophilic phosphine ligand in DMSO-$d_6$. (Peaks: -16.20 and 21.58 ppm)

**3. Crystal data**

The X-ray data for single crystals of Pd complex was obtained in a Bruker CCD X8 Kappa APEX II diffractometer outfitted with a graphite monochromator and Mo-Kα radiation (λ = 0.71073 Å). A combination of φ and ω scans was carried out to obtain at least a unique data set. The crystal structure was solved using direct methods in the SHELXS Fourier synthesis.[1] Anisotropic displacement parameters were applied to all non-hydrogen atoms, followed by full-matrix program. The final structure was refined using SHELXL, where the remaining atoms were located from difference least-squares refinement based on F. All hydrogen atoms were placed in ideal positions and refined as riding atoms with relative isotropic displacement parameters. The crystallographic data and structure refinement parameters for Pd complex are provided in Table S1. CCDC-1440920 contains the supplementary crystallographic data. These data can be obtained free of charge from The Cambridge Crystallographic Data Centre via www.ccdc.cam.ac.uk/data_request/cif

**Table S1** Crystallographic data and structure refinement parameters for **2**

| Molecular Formula | $C_{44}H_{48}Cl_2F_{12}N_6O_8P_2Pd_1S_4$ |
|---|---|
| Fw [g mol$^{-1}$] | 1384.36 |
| T [K] | 293 (2) |
| Wavelength [Å] | 0.71073 |
| Crystal system | Monoclinic |
| Space group | *P21/n* |
| *a* [Å] | 18.0287 (11) |
| *b* [Å] | 8.6686 (5) |
| *c* [Å] | 19.3834 (12) |
| *α* [°] | 90 |
| *β* [°] | 115.664 (2) |
| *g* [°] | 90 |
| V [Å$^3$] | 2730.5 (4) |
| *Z'* | 2 |
| $\rho_{calc}$ [g cm$^{-3}$] | 1.684 |
| $\mu$ [mm$^{-1}$] | 0.747 |
| *F*(000) | 1400 |
| Crystal size [mm] | 0.31 x 0.21 x 0.08 |
| $\vartheta$ range [°] | 3.118 to 28.342 |
| Limiting indices (*h, k, l*) | -24 ≤ *h* ≤ 24 |
| | -11 ≤ *k* ≤ 11 |
| | -25 ≤ *l* ≤ 25 |
| Reflections collected | 151039 |

| | |
|---|---|
| Reflections unique [$R_{int}$] | 6823 [0.0441] |
| Completeness to $\vartheta_{max}$ [%] | 99.8 |
| Data / restraints / param. | 6823 / 0 / 358 |
| Absorption correction | Gaussian |
| Refinement method | Full-matrix least-squares on F2 |
| Min. and max. transmission | 0. 7457 and 0.7013 |
| $R_1$ [I > 2s(I)][a] | 0.0232 |
| $wR_2$ [I > 2s(I)][a] | 0.0550 |
| $R_1$ (all data)[a] | 0.0279 |
| $wR_2$ (all data)[a] | 0.0574 |
| S on $F^2$[a] | 1.060 |
| Largest diff. peak and hole (e $Å^{-3}$) | 0.500 and -0.412 |

[a] As defined by the SHELXL program

**Table S2**. Selected bond lengths (Å) and angles (°)

| Bond lengths | | Bond angles | |
|---|---|---|---|
| Pd-P | 2.3255(4) | Cl-Pd-P | 87.557(12) |
| Pd-Cl | 2.3041(4) | Cl-Pd-P' | 92.442(12) |

Symmetry transformations used to generate equivalent atoms: ( ' ) -x,-y,-z

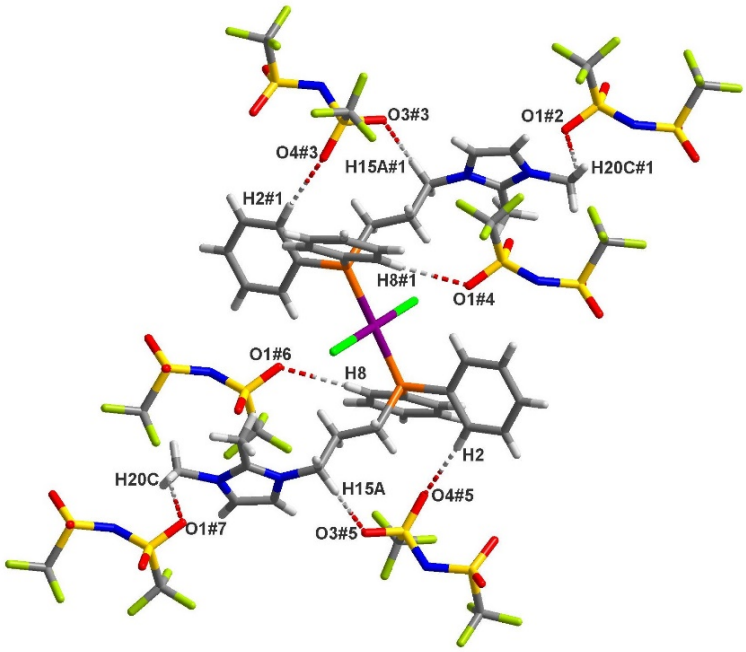


**Figure S3.** View of the intermolecular hydrogen-bond interactions between the ionophilic ligands and the $NTf_2^-$ anions in complex.

**Table S3.** Hydrogen bonds with H..A < r(A) + 2.000 Angstroms and <DHA > 110 deg. Observed for complex

| D-H | d(D-H) | d(H..A) | <DHA | d(D..A) | A |
|---|---|---|---|---|---|
| C2-H2 | 0.930 | 2.498 | 173.11 | 3.424 | O4 [ x, y-1, z-1 ] |
| C8-H8 | 0.930 | 2.579 | 138.15 | 3.330 | O1 [ x-1/2, -y+1/2, z-3/2 ] |
| C14-H14A | 0.970 | 2.856 | 123.95 | 3.491 | Cl [ -x, -y, -z ] |
| C15-H15A | 0.970 | 2.546 | 136.76 | 3.320 | O3 [ x, y-1, z-1 ] |
| C15-H15B | 0.970 | 2.828 | 163.99 | 3.770 | Cl [ x, y-1, z ] |
| C19-H19C | 0.960 | 2.976 | 146.22 | 3.811 | Cl [ x, y-1, z ] |
| C20-H20C | 0.960 | 2.533 | 144.32 | 3.360 | O1 [ x-1/2, -y-1/2, z-3/2 ] |

## 4. Computation details

The Pd(II) complex structure was extracted from its Crystallographic Information File (CIF). Frontier molecular orbitals were calculated using density functional theory (DFT) with ωB97X-D exchange-correlation functional, employing the 6-311+G(d,p) set for light atoms and the cc-pVDZ-PP basis set with pseudopotential for palladium. Gaussian 16 was used for all calculations.[2] Topological analysis was performed using Multiwfn,[3] and Hirshfeld surface analysis was conducted with Crystal Explorer 17,[4] providing insights into key interactions, such as weak contacts and hydrogen bonding, crucial for the complex's stabilization.

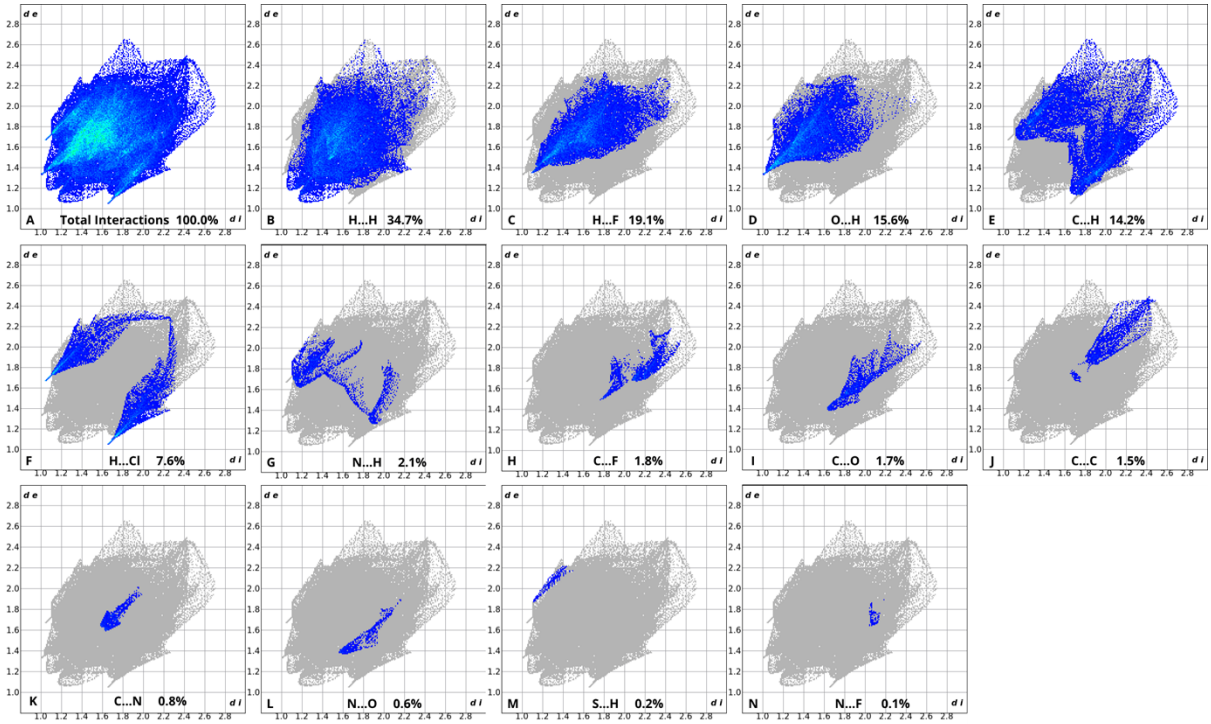


**Figure S4.** Quantification of intermolecular interactions in the Pd(II) complex through Hirshfeld surface analysis: (a) Total interaction; (b) H···H; (c) H···F; (d) O···H; (e) C···H; (f) H···Cl; (g) N···H; (h) C···F; (i) C···O; (j) C···C; (k) C···N; (l) N···O; (m) S···H; (n) N···F interactions.

Figure S2 quantifies the intermolecular interactions from the Hirshfeld surface analysis, revealing that the predominant interactions in the Pd(II) complex are H···H contacts, which account for 30% of the total interactions. A closer inspection of the hydrogen bonding interactions in Figures S2c and S2d highlights a concentration in the upper region of the plot, indicating the presence of non-classical hydrogen bonds.[5] Additionally, significant interactions, such as C···H contacts, contribute over 10% to the overall interactions.

Figure S3 illustrates the representation of bond paths and bond critical points (BCP) using Quantum Theory of Atoms in Molecules (QTAIM). These bond paths, shown in yellow, are critical in identifying interaction regions. The corresponding BCPs provide valuable insights into the electron density (ρ) at the interaction points, allowing us to categorize the strength of the interactions.

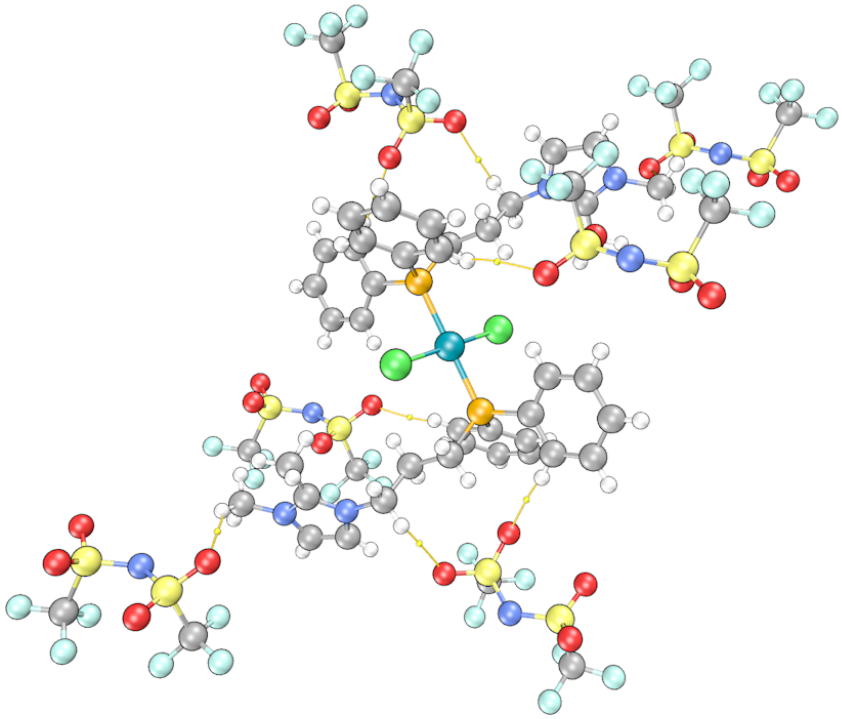

**Figure S5.** Bond paths and bond critical points (BCP) in the Pd(II) complex using Quantum Theory of Atoms in Molecules (QTAIM). Yellow lines represent bond paths, and small yellow spheres indicate bond critical points (BCP).

**Table S4.** QTAIM information for each hydrogen interaction. ρ(r) represents the electron density, $\nabla^2\rho$ the Laplacian of the electron density, and H(r) the energy density at the bond critical point (BCP). The intensity of the interactions is classified based on these values.

| Interaction | ρ(r) | $\nabla^2$ ρ(r) | H(r) | Intensity |
|---|---|---|---|---|
| O1#7-H20C | 0.00826439 | 0.0279944 | 0.00100369 | Weak |
| O3#5, H15A | 0.00787103 | 0.0278956 | 0.00108498 | Weak |
| O1#6, H8 | 0.00701954 | 0.0259947 | 0.00111678 | Weak |
| O4#5, H2 | 0.00296197 | 0.0120491 | 0.000708581 | Weak |
| O1#4, H8#1 | 0.00701954 | 0.0259947 | 0.00111678 | Weak |
| O4#3, H2#1 | 0.00718367 | 0.0266062 | 0.00120577 | Weak |
| O3#3, H15A#1 | 0.00787103 | 0.0278956 | 0.00108498 | Weak |
| O1#2, H20C#1 | 0.00826439 | 0.0279944 | 0.00100369 | Weak |

Table S3 presents the QTAIM data for each hydrogen interaction. The electron density ρ(r), its Laplacian $\nabla^2\rho(r)$, and the energy density H(r) at the BCPs were analyzed. Following the criteria proposed by Rozas et al. , hydrogen bonds are classified based on these values.[6] When

$\nabla^2\rho > 0$ and $H(r) > 0$, the bond is considered weak. Moderate hydrogen bonds are characterized by $\nabla^2\rho > 0$ and $E(r) < 0$, while strong hydrogen bonds are identified by $\nabla^2\rho < 0$ and $H(r) < 0$.

The analysis reveals symmetry in the interactions listed in Table S3. Specifically, pairs such as (O1#7-H20C and O1#2-H20C#1), (O3#5-H15A and O3#3-H15A#1), (O4#5-H2 and O4#3-H2#1), and (O1#6-H8 and O1#4-H8#1) are equivalent, resulting in four unique hydrogen bonds. These hydrogen bonds are weak to moderate, consistent with the non-classical hydrogen bonding suggested by the Hirshfeld surface analysis.

**5. DFT calculations**

In this work DFT-based calculations[5] were performed by the Vienna Ab initio Simulation Package (VASP 5.4.1)[7-8] which treats the interactions between ions and electrons by the projector augmented wave method (PAW).[9] The generalized gradient approximation (GGA) with the Perdew–Burke–Ernzerhof (PBE) exchange-correlation functional[10] was used in this study with a kinetic cut-off energy of 500 eV. The Brillouin zone for such molecular system was sampled considered only the $\Gamma$ k-point. The system under investigation was placed at the center of a 35 Å lattice cubic box with a minimum vacuum space between two neighboring systems of more than 15 Å to avoid possible interactions between periodic images. Here, we have considered a 55-atom icosahedron Pd nanoparticles (NP) with a diameter of ~1.05 nm. For metallic nanoparticles, the icosahedral structure is lower in energy than other symmetric structures.[11-12] All atoms were allowed to relax without constraints and the geometry optimization was stopped when the electronic energy tolerance ($10^{-7}$ eV) was reached, and the residual forces on each atom were less than 0.01 eV/Å. The van der Waals interactions (vdW) were included by using the semi-empirical D2 method.[13] The adsorption energy was calculated using the expression:

$$E(ads) = E(\text{Pd-NP + molecule}) - [E(\text{Pd-NP}) + E(\text{molecule})],$$

Where E(Pd-NP + molecule) is the total energy of the optimized system, E(Pd-NP) is the total energy of the icosahedral Pd-55 cluster and E(molecule) is the total energy of the isolated molecule. Thus, a negative E(ads) value means an exothermic adsorption of the molecule on the Pd-55 cluster.

For our system the largest ENMAX is 400 eV (to both carbon and nitrogen atoms of the ligands). Once the adsorption energy is essentially a difference of total energies to ensure a good compromise between computational cost and accuracy we have taken 500 eV for ENCUT.

To illustrate, we present below a table of the total energy for the isolated Pd-nanoparticle (55 atoms) as a function of the energy cutoff.

| **ENCUT** | **TOTAL ENERGY** | **\|ENERGY-DIFF\|** |
|---|---|---|
| 400 eV | -251.90047938 eV | ---------- |
| 500 eV | -251.93587959 eV | 0.0354 eV |
| 600 eV | -251.94442100 eV | 0.0085 eV |

Such results indicate that considering an ENCUT of 500 eV is enough to reach a good estimation of the adsorption energies.

The charge density difference (CDD) can be used to describe the electron transfer at the interface between the phosphine ligand and the nanoparticle, which is calculated as:

$$CDD= \rho_{AB} - \rho_A - \rho_B$$

where $\rho_{AB}$ is charge density calculated for the whole system, $\rho_A$ is charge density for the phosphine ligand and $\rho_B$ is charge density of Pd-nanoparticle.

**6. TOF calculations**

We have used the classical and extensively employed “number” of surface metal atoms

*The body volume of the Pd NPs was considered fcc,*

$$TON= \frac{n_{product}}{n_{Pd} \text{ x surface Pd \%}}$$

*% of number of surface Pd atom= $V_{shell}/V_{NPs}$*

*Volume of NPs= 4/3 p x $r^3$ NPs*

*Radius of Pd NPs (r)=1/2xdiameter*

*Shell volume containing Pd atoms was obtained as reported earlier.”*

## 7. Literature comparison of semi-hydrogenation of 1,3-cyclohexadiene in ionic liquid catalytic system

**Table S5:** Semi-hydrogenation driven by our phosphine-modified Pd NPs in comparison with literature

| Entry | Cat | Media | T ( °C) | $pH_2$( bar) | TOF [$s^{-1}$] | Ref. |
|---|---|---|---|---|---|---|
| **1** | **Pd NPs** | **BMIm.$NTf_2$** | **40** | **2.0** | **12.82** | **our** |
| 2 | PdNPs | BMIm.$PF_6$/phen | 40 | 1.0 | 0.07 | 14 |
| 3 | Pd NPs/phen- | SILP-TMGL ionic liquid | 20 | - | 0.33 | 15 |
| 4 | Pd NPs | 1,1,3,3-tetramethylguanidine trifluoroacetic acid (IL) | 60 | 20.0 | - | 16 |
| 5 | [Rh(COD)($PPh_3$)$_2$]$NTf_2$ | BMIm.$NTf_2$/ $CH_3CN$ | 30 | 1.2 | - | 17 |
| 6 | Ru NPs | BMIm.$NTf_2$ | 30 | 1.2 | 0.96 | 18 |
| 7 | Ru NPs | BMIm.$NTf_2$ | 30 | 1.2 | - | 19 |
| 8 | Pd NPs | D-MPIL.$NTf_2$/ Ethanol | 40 | 4.0 | 1.6 | 20 |
| 9 | Pd NPs | BMIm.$BF_4$/Phenosphines | 40 | 4.0 | - | 21 |
| 10 | Pd NPs/SILP-$Al_2O_3$ | $CH_2Cl_2$ | 40 | 4.0 | 20.1 | 22 |
| 11 | Pd NPs/ SILP-$SiO_2$ | $CH_2Cl_2$ | 40 | 5.0 | 3.0 | 23 |
| 12 | Pd/SILP-$SiO_2$ | CH2Cl2 | 40 | 4.0 | 3.03 | 24 |
| 13 | Au/ SILP-$Al_2O_3$ | n-hexane | 100 | 25.0 | 0.068 | 25 |
| 14 | Pd/poly(amidoamine) | CHCl3/methanol | 100 | - | 1.1 | 26 |

**SILP= Supported ionic liquid phases

## 8. References


1. Sheldrick, G., A short history of SHELX. *Acta Crystallogr. A* **2008,** *64* (1), 112-122.
2. M.J. Frisch, G. W. T., H.B. Schlegel, G.E. Scuseria, M.A. Robb, J.R. ; Cheeseman, G. S., V. Barone, G.A. Petersson, H. Nakatsuji, X. Li, M. ; Caricato, A. V. M., J. Bloino, B.G. Janesko, R. Gomperts, B. Mennucci, H.P. ; Hratchian, J. V. O., A.F. Izmaylov, J.L. Sonnenberg, D. Williams-Young, F. ; Ding, F. L., F. Egidi, J. Goings, B. Peng, A. Petrone, T. Henderson, D. ; Ranasinghe, V. G. Z., J. Gao, N. Rega, G. Zheng, W. Liang, M. Hada, M. ; Ehara, K. T., R. Fukuda, J. Hasegawa, M. Ishida, T. Nakajima, Y. Honda, O. ; Kitao, H. N., T. Vreven, K. Throssell, J.A. Montgomery Jr., J.E. Peralta, F. ; Ogliaro, M. J. B., J.J. Heyd, E.N. Brothers, K.N. Kudin, V.N. Staroverov, T. ; A. Keith, R. K., J. Normand, K. Raghavachari, A.P. Rendell, J.C. Burant, S. ; S. Iyengar, J. T., M. Cossi, J.M. Millam, M. Klene, C. Adamo, R. Cammi, J.W. ;

Ochterski, R. L. M., K. Morokuma, O. Farkas, J.B. Foresman, D.J. Fox, ; , Gaussian16 Revision C.01. **2016**.
3. Lu, T.; Chen, F., Multiwfn: A multifunctional wavefunction analyzer. *J. Comput. Chem.* **2012,** *33* (5), 580-592.
4. SM. J. Turner, J. J. M., S. K. Wolff, D. J. Grimwood, P. R. Spackman, D. Jayatilaka and M. A. Spackman, *CrystalExplorer17*. University of Western Australia: 2017.
5. Almeida, L. R.; Anjos, M. M.; Ribeiro, G. C.; Valverde, C.; Machado, D. F. S.; Oliveira, G. R.; Napolitano, H. B.; de Oliveira, H. C. B., Synthesis, structural characterization and computational study of a novel amino chalcone: a potential nonlinear optical material. *New J. Chem.* **2017,** *41* (4), 1744-1754.
6. Rozas, I.; Alkorta, I.; Elguero, J., Behavior of Ylides Containing N, O, and C Atoms as Hydrogen Bond Acceptors. *J. Am. Chem. Soc.* **2000,** *122* (45), 11154-11161.
7. Kresse, G.; Hafner, J., Ab initio molecular dynamics for liquid metals. *Phys. Rev. B* **1993,** *47* (1), 558-561.
8. Kresse, G.; Hafner, J., Ab initio molecular-dynamics simulation of the liquid-metal--amorphous-semiconductor transition in germanium. *Physical Review B* **1994,** *49* (20), 14251-14269.
9. Kresse, G.; Joubert, D., From ultrasoft pseudopotentials to the projector augmented-wave method. *Phys. Rev. B* **1999,** *59* (3), 1758-1775.
10. Becke, A. D., Density-functional exchange-energy approximation with correct asymptotic behavior. *Physical Review A* **1988,** *38* (6), 3098-3100.
11. Karabacak, M.; Özçelik, S.; Güvenç, Z. B., Structures and energetics of Pd21–Pd55 clusters. *Surf. Sci.* **2003,** *532-535*, 306-311.
12. Zhu, J.; Cheng, P.; Wang, N.; Huang, S., Insight into the structural and electronic properties of Pd55−nNin (n=0–55) clusters: A density functional theory study. *Comput. Theor. Chem.* **2015,** *1071*, 9-17.
13. Grimme, S., Semiempirical GGA-type density functional constructed with a long-range dispersion correction. *J. Comput. Chem.* **2006,** *27* (15), 1787-1799.
14. Huang, J.; Jiang, T.; Han, B.; Gao, H.; Chang, Y.; Zhao, G.; Wu, W., Hydrogenation of olefins using ligand-stabilized palladium nanoparticles in an ionic liquid. *Chem. Commun.* **2003,** (14), 1654-1655.
15. Huang, J.; Jiang, T.; Gao, H.; Han, B.; Liu, Z.; Wu, W.; Chang, Y.; Zhao, G., Pd Nanoparticles Immobilized on Molecular Sieves by Ionic Liquids: Heterogeneous Catalysts for Solvent-Free Hydrogenation. *Angew. Chem. Int. Ed.* **2004,** *43* (11), 1397-1399.
16. Tao, R.; Miao, S.; Liu, Z.; Xie, Y.; Han, B.; An, G.; Ding, K., Pd nanoparticles immobilized on sepiolite by ionic liquids: efficient catalysts for hydrogenation of alkenes and Heck reactions. *Green Chemistry* **2009,** *11* (1), 96-101.
17. Campbell, P. S.; Podgoršek, A.; Gutel, T.; Santini, C. C.; Pádua, A. A. H.; Costa Gomes, M. F.; Bayard, F.; Fenet, B.; Chauvin, Y., How do Physical−Chemical Parameters Influence the Catalytic Hydrogenation of 1,3-Cyclohexadiene in Ionic Liquids? *J. Phys. Chem. B* **2010,** *114* (24), 8156-8165.
18. Campbell, P. S.; Santini, C. C.; Bayard, F.; Chauvin, Y.; Collière, V.; Podgoršek, A.; Costa Gomes, M. F.; Sá, J., Olefin hydrogenation by ruthenium nanoparticles in ionic liquid media: Does size matter? *J. Catal.* **2010,** *275* (1), 99-107.
19. Salas, G.; Campbell, P. S.; Santini, C. C.; Philippot, K.; Costa Gomes, M. F.; Pádua, A. A. H., Ligand effect on the catalytic activity of ruthenium nanoparticles in ionic liquids. *Dalton transactions* **2012,** *41* (45), 13919-13926.

20. Simon, N. M.; Abarca, G.; Scholten, J. D.; Domingos, J. B.; Mecerreyes, D.; Dupont, J., Structural, electronic and catalytic properties of palladium nanoparticles supported on poly(ionic liquid). *Appl. Catal. A: Gen.* **2018,** *562*, 79-86.
21. Leal, B. C.; Consorti, C. S.; Machado, G.; Dupont, J., Palladium metal nanoparticles stabilized by ionophilic ligands in ionic liquids: synthesis and application in hydrogenation reactions. *Catal. Sci. Technol.* **2015,** *5* (2), 903-909.
22. Luza, L.; Gual, A.; Eberhardt, D.; Teixeira, S. R.; Chiaro, S. S. X.; Dupont, J., "Imprinting" Catalytically Active Pd Nanoparticles onto Ionic-Liquid-Modified Al2O3 Supports. *ChemCatChem* **2013,** *5* (8), 2471-2478.
23. Luza, L.; Rambor, C. P.; Gual, A.; Bernardi, F.; Domingos, J. B.; Grehl, T.; Brüner, P.; Dupont, J., Catalytically Active Membranelike Devices: Ionic Liquid Hybrid Organosilicas Decorated with Palladium Nanoparticles. *ACS Catal.* **2016,** *6* (10), 6478-6486.
24. Luza, L.; Gual, A.; Rambor, C. P.; Eberhardt, D.; Teixeira, S. R.; Bernardi, F.; Baptista, D. L.; Dupont, J., Hydrophobic effects on supported ionic liquid phase Pd nanoparticle hydrogenation catalysts. *Phys. Chem. Chem. Phys.* **2014,** *16* (34), 18088-18091.
25. Luza, L.; Rambor, C. P.; Gual, A.; Alves Fernandes, J.; Eberhardt, D.; Dupont, J., Revealing Hydrogenation Reaction Pathways on Naked Gold Nanoparticles. *ACS Catal.* **2017,** *7* (4), 2791-2799.
26. Mizugaki, T.; Murata, M.; Fukubayashi, S.; Mitsudome, T.; Jitsukawa, K.; Kaneda, K., PAMAM dendron-stabilised palladium nanoparticles: effect of generation and peripheral groups on particle size and hydrogenation activity. *Chem. Commun.* **2008,** (2), 241-243.